Geophysical Research Letters

RESEARCH LETTER
10.1029/2019GL082969

Controls on the Width of Tropical Precipitation and Its Contraction Under Global Warming

A. Donohoe[1], A. R. Atwood[2], and M. P. Byrne[3,4]

[1]Polar Science Center, Applied Physics Laboratory, University of Washington, Seattle, WA, USA, [2]Department of Earth Ocean and Atmospheric Science, Florida State University, Tallahassee, FL, USA, [3]School of Earth and Environmental Sciences, University of St. Andrews, St. Andrews, UK, [4]Department of Physics, University of Oxford, Oxford, UK

Key Points:
- The seasonal range of ITCZ migrations (SR_{ITCZ}) controls the meridional extent of tropical precipitation
- SR_{ITCZ} is larger than observed in most climate models resulting in a double-ITCZ bias
- Under global warming, SR_{ITCZ} decreases due to more efficient cross-equatorial heat transport and tropical precipitation contracts

Supporting Information:
- Supporting Information S1
- Figure S1
- Figure S2
- Figure S3
- Figure S4

Correspondence to:
A. Donohoe,
thedhoe@gmail.com;
adonohoe@u.washington.edu

Citation:
Donohoe, A., Atwood, A. R., & Byrne, M. P. (2019). Controls on the width of tropical precipitation and its contraction under global warming. *Geophysical Research Letters*, *46*, 9958–9967. https://doi.org/10.1029/2019GL082969

Received 26 MAR 2019
Accepted 20 JUN 2019
Accepted article online 28 JUN 2019
Published online 29 AUG 2019

Abstract Climate models robustly and unanimously simulate narrowing of the intense tropical precipitation under greenhouse gas forcing. We argue that the meridional width of tropical precipitation is controlled by the seasonal meridional range of the Intertropical Convergence Zone (ITCZ). The contraction of tropical precipitation under greenhouse forcing results from a reduced seasonal range of ITCZ migration. An energetic theory—similar to the energetic theory for ITCZ shifts based on the hemispheric contrast of energy input to the atmosphere—is developed. The meridional width of tropical precipitation is proportional to the seasonal range of the interhemispheric contrast in atmospheric heating divided by the efficiency of atmospheric cross-equatorial heat transport. Climate models are biased toward overly expansive tropical precipitation resulting from an exaggerated seasonal atmospheric heating. The robust contraction of tropical precipitation under global warming results from increased efficiency of interhemispheric energy transport consistent with enhanced gross moist stability of the tropical atmosphere.

1. Introduction

Contractions and expansions of the tropical region have widespread impacts on agricultural productivity, especially in semiarid regions where water resources are marginal. There is a general consensus in the literature that the arid regions of the Earth have expanded poleward over the satellite record (Johanson & Fu, 2009; Quan et al., 2014). Previous studies have primarily focused on the poleward extent of the arid regions where there is subsiding motion in the Hadley circulation and the relative impacts of natural variability and anthropogenic forcing is unclear (Waugh et al., 2015). Here, we focus on the meridional extent of intense tropical precipitation in the Intertropical Convergence Zone (ITCZ)—hereafter the width of annual tropical precipitation (WA_{ITCZ})—which is associated with the ascending branch of the Hadley circulation. Previous work has demonstrated that WA_{ITCZ} over the Pacific has contracted in recent decades (Wodzicki & Rapp, 2016) and robustly contracts in climate models under increased atmospheric CO_2 concentrations (Byrne & Schneider, 2016a; Lau & Kim, 2015) although the proposed mechanisms involve competing effects from transient-eddy energy fluxes (Byrne & Schneider, 2016b), gross moist stability of the tropics (Byrne & Schneider, 2016a; Chou et al., 2009), and cloud radiative effects (Su et al., 2017). We note that while other studies have defined the ITCZ width as the tropical region of upwelling atmospheric motion (Byrne & Schneider, 2016a; Lau & Kim, 2015), we focus on the meridional distance between the tropical precipitation peaks in each hemisphere that was previously identified as the "distance between the two ITCZs" (Popp & Lutsko, 2017).

The ITCZ migrates between 8°N in the boreal summer and 6°S in the austral summer (Chiang & Friedman, 2012; Donohoe, Marshall, Ferreira, & McGee, 2013), and it has long been realized that the annual mean precipitation is shaped by this seasonal migration (Hadley, 1735); loosely speaking, regions within the seasonal march of the ITCZ are moist whereas those outside are dry (Sachs et al., 2009). Here, we explicitly examine the relationship between the seasonal migration of the ITCZ and WA_{ITCZ} and demonstrate that WA_{ITCZ} is controlled by the seasonal range of the ITCZ migrations. We apply this insight to two key problems in tropical climate dynamics:

Double ITCZ bias. The climate model bias toward an overly wide WA_{ITCZ} (the double ITCZ bias) is a consequence of an exaggerated seasonal range of ITCZ migration.

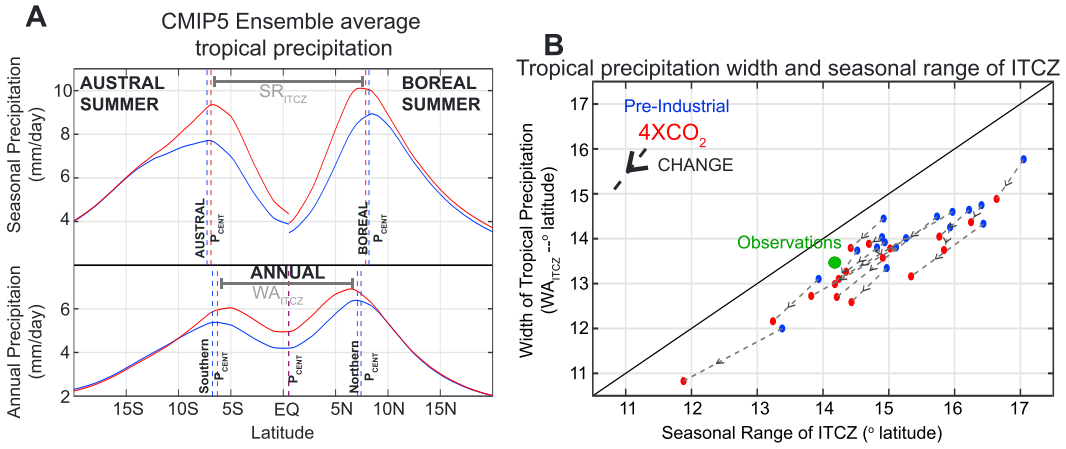

Figure 1. (a) Ensemble mean precipitation in (blue) preindustrial and (red) $4XCO_2$ simulations. Austral summer is shown in the upper left, Boreal summer in the upper right with vertical lines representing the seasonal Intertropical Convergence Zone (ITCZ) location. The annual mean is shown in the bottom panel with vertical dashed lines representing the tropical, Northern, and Southern P_{CENT}. (b) Scatter plot of SR_{ITCZ} versus WA_{ITCZ}. Blue and red dots represent the PI and $4XCO_2$ values in individual models, respectively, and arrows indicate the change. Observational values are shown by the green dot. The black line is the 1:1 line.

Tropical contraction under global warming. The robust contraction of WA_{ITCZ} under CO_2 forcing results from a decrease in the seasonal range of ITCZ migration.

2. Tropical Precipitation Width and the Seasonal Migration of the ITCZ

In general, the annual- and zonal-mean tropical precipitation in CMIP5 (Taylor et al., 2012) models is bimodal with maxima centered around 7° north and south and a weak local minimum near the equator (bottom panel of Figure 1a). This bimodality is the time average of a single-peaked precipitation distribution sinusoidally following the insolation with the local minimum occurring in the equatorial region where the ITCZ rapidly passes overhead (Hu et al., 2007; Xian & Miller, 2008). The local extrema occur in the locations where the ITCZ lingers in vicinity of the edge of the annual range and the width between the modal locations is set by the seasonal range of ITCZ migration.

A common metric of the annual mean ITCZ location is the precipitation centroid (P_{CENT}), defined as the latitude delineating regions of equal area weighted precipitation between 20°S and 20°N (Frierson & Hwang, 2012). P_{CENT} is preferred over defining the ITCZ as the location of peak precipitation because P_{CENT} accommodates bimodal precipitation distributions (Bordoni & Schneider, 2008) where picking a single peak is problematic and is sensitive to model grid spacing. We expand on this metric by defining two additional quantities relevant to the width of tropical precipitation (see the supporting information for methodological details and Figure S2 for a visual demonstration of metrics): (1) The seasonal range of the ITCZ (SR_{ITCZ}) defined as the centroid of July–August (JA) precipitation minus that in January–February (JF) and (2) the width of annual precipitation (WA_{ITCZ}) defined as the centroid of annual mean precipitation to the north of P_{CENT} (northern P_{CENT}) minus that defined to the south of P_{CENT} (southern P_{CENT}). We note that alternative metrics for ITCZ location, including precipitation (raised to a power) weighted latitude (Adam et al., 2016), yield similar results to the P_{CENT} metrics used here (not shown).

In CMIP5 preindustrial (PI) simulations WA_{ITCZ} varies substantially across models (between 12° and 16°) and all but three of the models have larger WA_{ITCZ} than observed (13.4°, Figure 1b). Model biases in WA_{ITCZ} and SR_{ITCZ} relative to the observations are negligibly impacted by anthropogenic forcing since the PI period (Figure S1). As expected, SR_{ITCZ} and WA_{ITCZ} are strongly ($R = 0.91$) correlated with a regression coefficient near unity (1.03), suggesting that the location of the annual mean precipitation peak in each hemisphere is a consequence of the ITCZ location during the local summer as opposed to the bimodality of the precipitation during a given season. In all models the SR_{ITCZ} exceeds the WA_{ITCZ} (values fall below the 1:1 line in Figure 1b), which is expected since the time average precipitation maxima cannot be farther off the equator than the seasonal extremes of ITCZ migration.

The above results indicate that the climate model bias toward a more meridionally expansive and bimodal tropical precipitation distribution is a consequence of biases toward larger SR_{ITCZ}, and we equate this bias with the terminology "double ITCZ." Our definition differs from that in recent literature (Hwang & Frierson, 2013) that equates the double ITCZ bias with the contrast in tropical precipitation between the two hemispheres. We will argue that there are two independent modes of tropical precipitation biases: (1) the hemispheric contrast in annual mean tropical precipitation that results from the *annual mean* ITCZ location documented by Hwang and Frierson (2013) and (2) the width or degree of bimodality (WA_{ITCZ}) in the tropical precipitation that is governed by the SR_{ITCZ} and is the focus of the current work.

In response to a quadrupling of CO_2, all 17 of the CMIP5 models simulate an intensification of tropical precipitation and a contraction of WA_{ITCZ} (an ensemble average change of 5% from 14.0° to 13.3°; Byrne & Schneider, 2016a; Lau & Kim, 2015; Su et al., 2017) characterized by a pinching of the two annual mean tropical precipitation maximums toward the equator (lower panel of Figure 1a). The reduced WA_{ITCZ} under global warming results from a 5% reduction in SR_{ITCZ} (from 15.4° to 14.6°; upper panel of Figure 1a). In all climate models, both the WA_{ITCZ} and SR_{ITCZ} decrease under $4XCO_2$ as can be seen from the arrows connecting the PI and $4XCO_2$ values in each climate model pointing down and left. Furthermore, the SR_{ITCZ} reduction under global warming is well correlated ($R = 0.89$) with the decrease in WA_{ITCZ} across the models with a regression coefficient near unity (1.1). These results are consistent with the findings of Huang et al. (2013) that seasonal precipitation changes under global warming are centered equatorward of the climatological precipitation.

These results collectively demonstrate that WA_{ITCZ} and its change due to external forcing is tightly linked to SR_{ITCZ}. In the next section, we develop a theory for SR_{ITCZ} with the aim of understanding both mean state biases and changes under global warming.

3. Mechanisms Controlling Tropical Precipitation Width

We begin our discussion of mechanisms controlling the WA_{ITCZ} using an ensemble of idealized simulations performed using the GFDL AM2.1 model where we modify the amplitude of the seasonal cycle of atmospheric temperature (Donohoe, Frierson, & Battisti, 2013). In these simulations, the atmosphere is coupled to a slab ocean that covers the entire planet (aquaplanet) and the slab depth is globally uniform but varies between the five ensemble members from 2.4 to 50 m. When the ocean is deep, ocean temperatures change little in response to seasonal changes in insolation. As a result, the sea surface temperature (SST) maximum remains near the equator at all times of year, the seasonal ITCZ migration is limited and the annual mean precipitation is singly peaked near the equator (dark blue line in Figure 2a). In simulations with a shallower mixed layer depth, the same seasonal variations in insolation result in much more heating of the surface and adjacent atmosphere such that the temperature maximum and ITCZ migrate off the equator. As a result the annual mean precipitation is smeared across a wider range of latitudes resulting in a bimodal precipitation distribution at intermediate depths and nearly uniform weak tropical precipitation at shallow depths. The WA_{ITCZ} increases alongside the SR_{ITCZ} with decreasing ocean depth (Figure 2a). Inspired by this idealized example of how the amplitude of the seasonal cycle controls the distribution of annual mean precipitation, we seek a theory for the SR_{ITCZ}.

An energetic theory for the annual mean ITCZ location has emerged in recent literature (Kang et al., 2008; Schneider et al., 2014), and motivated by its success, we extend this theory to analyze SR_{ITCZ}. The starting point for this theory is that the interhemispheric atmospheric energy transport and tropical precipitation are both intimately linked to the Hadley cell location; the precipitation is colocated with the ascending branch of the Hadley Cell and the atmospheric energy transport is in the direction of motion in the upper branch of the Hadley cell such that the atmosphere fluxes energy across the equator (AHT_{EQ}) away from the ITCZ with a magnitude proportional to the ITCZ displacement off the equator (Donohoe, Marshall, Ferreira, & McGee, 2013). Thus, the ITCZ location (Frierson et al., 2013; Hwang & Frierson, 2013; Marshall et al., 2013) and its migration due to external forcing (Frierson & Hwang, 2012) is tightly linked to the AHT_{EQ} demanded by the hemispheric contrast of atmospheric heating.

AHT_{EQ} and ITCZ location are highly ($R^2 = 0.99$) correlated over the observed (and modeled) climatological seasonal cycle (Donohoe, Marshall, Ferreira, & McGee, 2013). We use this near-perfect seasonal correlation to express the SR_{ITCZ} in terms of the seasonal range of AHT_{EQ}—denoted by $\left\|AHT_{EQ}\right\|$, where vertical

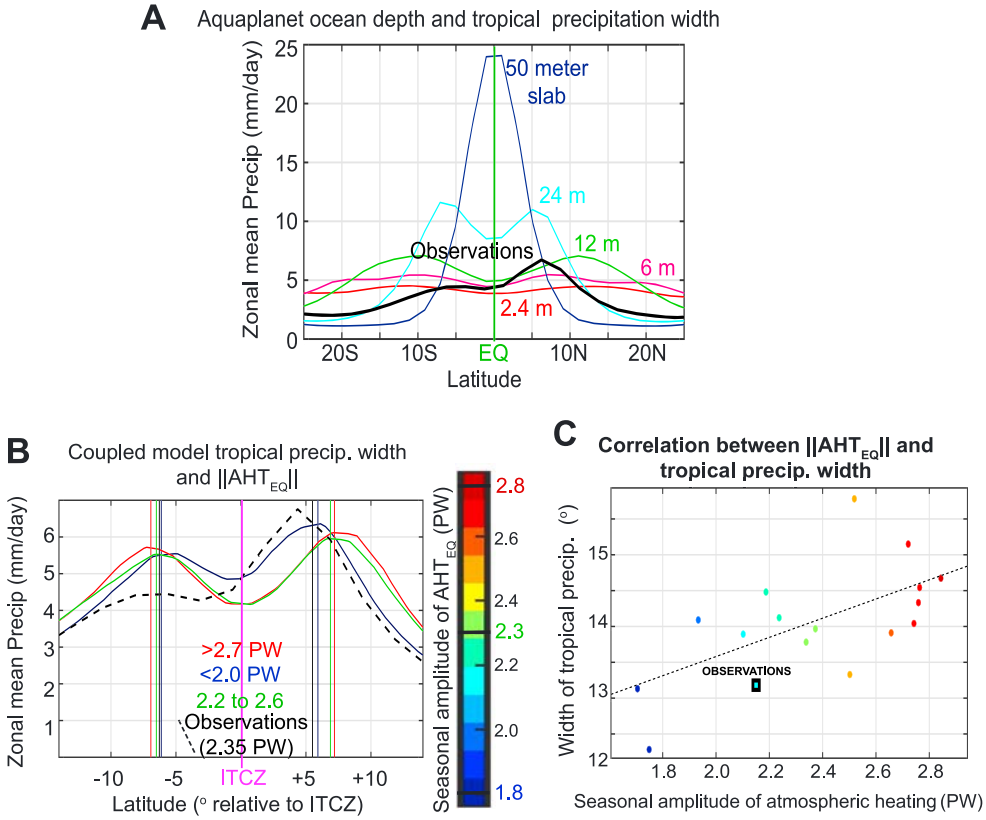

Figure 2. (a) Annual mean precipitation in aquaplanet simulations with varying mixed layer depth. Observed precipitation is shown in black. (b) Zonal mean precipitation in CMIP5 PI models composited by large (>2.7 PW, red), medium (2.2–2.6 PW, green), and small (<2.0 PW, blue) $\left\|\mathrm{AHT_{EQ}}\right\|$. The observations are shown in the dashed black line and the color coding indicates $\left\|\mathrm{AHT_{EQ}}\right\|$ as shown in the color bar. Vertical lines show the locations of the Northern Hemisphere and Southern Hemisphere tropical precipitation centroids used to define $\mathrm{WA_{ITCZ}}$. (c) $\mathrm{WA_{ITCZ}}$ versus $\left\|\mathrm{AHT_{EQ}}\right\|$ in CMIP5 PI simulations. Observations are shown by the cyan square, and the dashed line shows the linear regression. ITCZ = Intertropical Convergence Zone.

brackets denote the amplitude of the annual harmonic—and the efficiency of $\mathrm{AHT_{EQ}}$ per unit of ITCZ shift ($\mathrm{EFF_{AHT}}$):

$$\mathrm{SR_{ITCZ}} = \frac{1}{\mathrm{EFF_{AHT}}}\left\|\mathrm{AHT_{EQ}}\right\|. \tag{1}$$

Equation (1) assumes that $\mathrm{EFF_{AHT}}$ is invariant over the seasonal cycle but can differ between climate models (and observations) and with climate state. This conceptual framework provides two possible mechanisms for changes and/or intermodel differences in $\mathrm{SR_{ITCZ}}$:

Changes in the magnitude of atmospheric heating/cooling during the solstitial seasons. If the atmosphere in the summer hemisphere receives more energy over the summer, the seasonal demand of $\mathrm{AHT_{EQ}}$ increases resulting in larger $\left\|\mathrm{AHT_{EQ}}\right\|$ and $\mathrm{SR_{ITCZ}}$ (provided $\mathrm{EFF_{AHT}}$ is unchanged). Though we have discussed this mechanism in terms of energy input to the summer hemisphere, the relevant metric driving $\mathrm{AHT_{EQ}}$ is the seasonal range of the hemispheric contrast of energy input to the atmosphere (defined as the amplitude of the annual harmonic—energy input to the atmosphere (defined as the amplitude of the annual harmonic—see section S2 in the supporting information).

Changes in $\mathrm{EFF_{AHT}}$. In the absence of changes in $\left\|\mathrm{AHT_{EQ}}\right\|$, an atmosphere with a larger $\mathrm{EFF_{AHT}}$ can achieve the same energy transport with a smaller Hadley cell/ITCZ displacement off the equator, which results in a smaller $\mathrm{SR_{ITCZ}}$.

We use this framework to understand the CMIP5 double ITCZ bias and contraction of $\mathrm{WA_{ITCZ}}$ under global warming in the next section. Before proceeding, we discuss the processes that control $\left\|\mathrm{AHT_{EQ}}\right\|$ and $\mathrm{EFF_{AHT}}$.

3.1. Processes Controlling the Seasonal Range of AHT_{EQ}–$\|AHT_{EQ}\|$

The required AHT_{EQ} at any instance is (Donohoe, Marshall, Ferreira, & McGee, 2013)

$$AHT_{EQ} = \langle SW_{ABS} \rangle + \langle SHF \rangle - \langle OLR \rangle - \langle STOR_{atmos} \rangle \quad (2)$$

where brackets indicate the spatial integral in the Southern Hemisphere (SH) minus that in the Northern Hemisphere (NH), SW_{ABS} is the shortwave absorption in the atmosphere, SHF is the upward flux of latent, sensible, and longwave radiation at the surface (note that the SHF does not include the surface solar radiation as this quantity is included in the atmospheric budget via the SWABS term), OLR is the outgoing longwave radiation and $STOR_{atmos}$ is the energy tendency in the atmospheric column. In the summer hemisphere, the atmosphere is heated from two sources: (1) the direct absorption of solar radiation in the atmospheric column by constituents such as ozone and water vapor and (2) the upward turbulent and longwave radiative energy fluxes from the surface as the ocean and land warm up in response to increased downwelling solar radiation at the surface. These sources of energy to the atmosphere are partly balanced by storage in the column ($STOR_{atmos}$) and enhanced OLR to space as the column heats up; the remainder of the excess energy is fluxed across the equator (AHT_{EQ}).

In the slab ocean aquaplanet simulations, the magnitude (and source) of seasonal heating of the atmosphere changes with mixed layer depth: (i) in simulations with a deeper ocean mixed layer, the summer atmosphere is heated primarily by $\langle SW_{ABS} \rangle$ since the intensification of downweliing solar radiation in the summer barely warms the high heat capacity ocean surface to drive upward SHF (Donohoe, Frierson, & Battisti, 2013), whereas (ii) in simulations with a shallower ocean, in addition to seasonal atmospheric heating provided by the (nearly mixed layer depth independent) $\langle SW_{ABS} \rangle$, downwelling solar radiation at the surface heats the ocean in the summer hemisphere resulting in greater upward turbulent energy fluxes that heat the atmosphere from below. Thus, the energetics demand a larger magnitude AHT_{EQ} during the solstice seasons in the shallower ocean simulations which results in a larger SR_{ITCZ} and wider WA_{ITCZ}.

Ocean mixed layer depth and the amount of solar radiation incident on the land and ocean surfaces—controlled by cloud properties—are expected to play a primary role in setting the seasonal amplitude of atmospheric heating at the hemispheric scale. Under global warming, the heating of the summer hemisphere by $\langle SW_{ABS} \rangle$ increases (Donohoe & Battisti, 2013) due to atmospheric moistening whereas the melting of sea ice exposes the atmosphere to the heat capacity of the ocean—akin to the deep slab ocean simulations—thereby reducing the seasonal heating of the atmosphere by surface turbulent energy fluxes (Dwyer et al., 2012).

3.2. Processes Setting the Efficiency of Cross-Equatorial Heat Transport

The $\frac{1}{EFF_{AHT}}$ in equation (1) is the seasonal slope of ITCZ location with respect to AHT_{EQ} that has been shown to be approximately 3° PW^{-1} (Donohoe, Marshall, Ferreira, & McGee, 2013); in order to move 1 PW of energy between the hemispheres via a cross-equatorial Hadley cell, the ITCZ must move 3° latitude into the opposing hemisphere. While this seasonal slope differs modestly between climate models, the approximate 3° PW^{-1} slope also aptly describes interannual ITCZ shifts (Donohoe, Marshall, Ferreira, Armour, & McGee, 2013) and long-term ITCZ shifts due to external forcing (Donohoe, Marshall, Ferreira, & McGee, 2013; Frierson & Hwang, 2012), since anomalies in ITCZ location are small compared to the climatological seasonal cycle (Donohoe & Voigt, 2015) and, thus, are governed by the seasonal slope. Notable exceptions to this rule have been found for cases where changes in annual mean AHT_{EQ} are not dominated by the Hadley cell (Roberts et al., 2017). We return to the processes that set EFF_{AHT} and its potential dependence on climate state below.

From a dynamics perspective, the AHT_{EQ} demanded energetically is accomplished by the zonal mean mass transport in the Hadley cell (Ψ_{EQ}) acting on the gross moist stability of the atmosphere at the equator (GMS_{EQ}) = $c_p\left(\theta_{e,\text{upper}} - \theta_{e,\text{lower}}\right)$—defined here as the specific heat capacity of air at constant pressure (c_p) times the equivalent potential temperature (θ) contrast between the poleward and equatorward flowing air in the upper and lower branches of the Hadley circulation, respectively (Czaja & Marshall, 2006; Held, 2001):

$$AHT_{EQ} \approx \Psi_{EQ} GMS_{EQ}, \quad (3)$$

where the approximation results from the assumption that eddies do not contribute to AHT_{EQ}. Equation (3) would constrain EFF_{AHT} for a given value of GMS_{EQ} if the relationship between ITCZ location and Ψ_{EQ} were

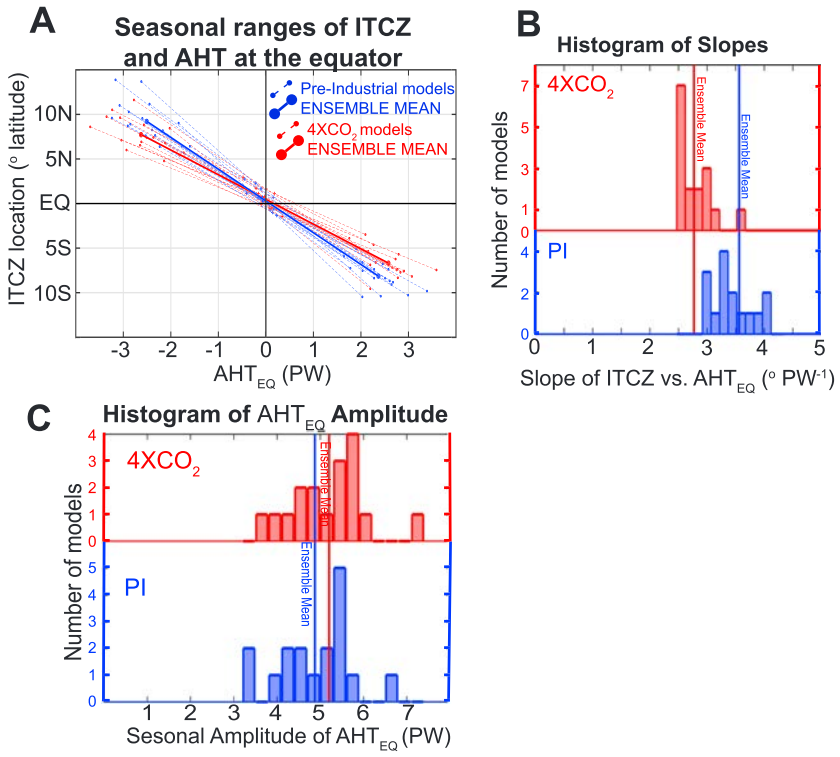

Figure 3. (a) The seasonal relationship between AHT_{EQ} (abscissa) and ITCZ location (ordinate—defined by the precipitation centroid) in CMIP5 PI (blue) and $4XCO_2$ (red) simulations. Each line is a different model with the length of the projection onto the abscissa equal to the seasonal amplitude of AHT_{EQ} ($\left\|AHT_{EQ}\right\|$) and the slope equal to the regression coefficient between ITCZ location and AHT_{EQ} (see introduction to section 4 for details). Histogram of (b) seasonal slopes and (c) $\left\|AHT_{EQ}\right\|$ for PI (blue) and $4XCO_2$ (red) simulations. ITCZ = Intertropical Convergence Zone.

known. While the magnitude of Ψ_{EQ} generally increases with increasing displacement of the ITCZ (and Hadley cell) off the equator, several factors influence the magnitude of the Ψ_{EQ} change per unit ITCZ shift: (i) the meridional gradient of the stream function (Ψ) between the ITCZ and the equator that itself steepens with ITCZ displacement off the equator as the winter Hadley cell intensifies (Lindzen & Hou, 1988) and (ii) the location of the ITCZ within the Hadley circulation (the ITCZ is near the zero stream function when the ITCZ is close to the equator and Hadley cells are symmetric around the equator but is located significantly within the winter Hadley cell when the ITCZ moves off the equator (Donohoe, Marshall, Ferreira, & McGee, 2013) and the winter cell intensifies). These complicating factors—and their potential changes with climate state—make the quantification and physical interpretation of EFF_{AHT} changes difficult. We diagnose and discuss changes in EFF_{AHT} more generally and note that, under global warming, increased GMS_{EQ} (Chou & Chen, 2010; Ma et al., 2012) favors enhanced EFF_{AHT} with all other factors being equal.

4. Controls on Tropical Precipitation Width in CMIP Models

The mechanisms controlling the SR_{ITCZ} discussed in the previous section can be visualized by plotting the seasonal cycles of the AHT_{EQ} and ITCZ location (Figure 3). In this figure, the projection of the line onto the abscissa is equal to $\left\|AHT_{EQ}\right\|$, and the slope is the regression coefficient between ITCZ location and AHT_{EQ} and is equivalent to $\frac{1}{EFF_{AHT}}$. Each line is centered on the annual mean AHT_{EQ} and ITCZ location. In the context of the mechanisms discussed above, the SR_{ITCZ} (ordinate range) can differ due to differences in the length of the abscissa (i.e., differences in the seasonal amplitude of atmospheric heating) with fixed slope or due to differences in the slope ($\frac{1}{EFF_{AHT}}$) with fixed seasonal atmospheric heating.

4.1. Cause of Double ITCZ Biases

The intermodel spread of SR_{ITCZ} in PI simulations results primarily ($R = 0.65$) from differences in $\left\|AHT_{EQ}\right\|$, whereas the slopes are not significantly correlated with SR_{ITCZ}; the blue lines in Figure 3 have similar slopes

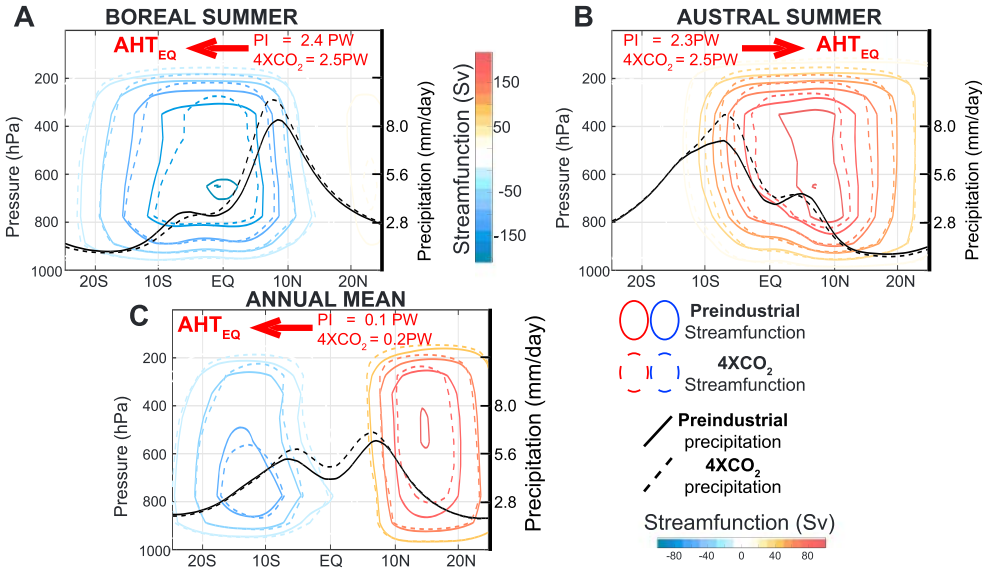

Figure 4. Mass overturning stream function (red and blue contours) and precipitation (black lines) for the CMIP5 PI (solid lines) and $4XCO_2$ (dashed lines) ensemble average. The red arrows and numbers show the AHT_{EQ} direction and magnitude. (a) The boreal summer (JA), (b) the austral (JF) summer, and (c) the annual mean all with stream function contour interval of 30 Sv (1 Sv = 10^9 kg/S) but with differing magnitude color scaling for the seasonal versus annual plots as shown by the color bars in the upper and lower panels.

but contrasting lengths (cf. the fractional ensemble spread of $\|AHT_{EQ}\|$ and slope in the histograms in Figures 3b and 3c). This result indicates that the intermodel spread in SR_{ITCZ} results from variations in the amplitude of seasonal atmospheric heating and not due to differences in EFF_{AHT}. Since, the SR_{ITCZ} is intimately linked to WA_{ITCZ}, intermodel differences in WA_{ITCZ} are significantly correlated ($R = 0.60$) with those in $\|AHT_{EQ}\|$ (Figure 2c).

To elaborate on this point, we composite the simulated annual mean precipitation in the PI control runs into three sets based on the value of $\|AHT_{EQ}\|$: (i) large seasonal cycle ($\|AHT_{EQ}\| > 2.7$ PW, red line in Figure 2b), (ii) moderate seasonal cycle (2.2 PW $< \|AHT_{EQ}\| < 2.6$ PW, green line), and (iii) small seasonal cycle ($\|AHT_{EQ}\| < 2.0$ PW, blue line). The tropical precipitation has wider separation between bimodal peaks in models with a large $\|AHT_{EQ}\|$ as compared to those with a small $\|AHT_{EQ}\|$ (cf. the red and blue precipitation profiles). The observed $\|AHT_{EQ}\|$ (2.35 PW) is smaller than that in most of the climate models (black square in Figure 2c) and the observed meridional profile of tropical precipitation better matches that of the small seasonal cycle composite (cf. the dashed black line with the dark blue in Figure 2b) with the added caveat that the hemispheric contrast between tropical precipitation in the NH and SH is larger in the observations than in the models.

4.2. Cause of Tropical Precipitation Contraction Under Global Warming

In response to CO_2 quadrupling, $\|AHT_{EQ}\|$ increases modestly in all 17 models with an ensemble average of 0.14 PW (≈6% of climatology)—favoring an enhanced SR_{ITCZ}—that is consistent with enhanced absorption of solar radiation in the summer hemisphere due to ice melting and increased absorption by water vapor in the moistened atmosphere (Donohoe et al., 2014). However, counteracting these modest changes in $\|AHT_{EQ}\|$, the seasonal slope between ITCZ location and AHT_{EQ} robustly (99.9% confidence interval) and unanimously (in all models) decreases (cf. the red and blue histograms in Figure 3b) indicating an enhanced EFF_{AHT} with global warming. The ensemble average slope decreases by 22% between PI and $4XCO_2$ from (-3.6 to $-2.8°$ PW^{-1}), favoring a reduced SR_{ITCZ}. As a result of the reduced $ITCZ/AHT_{EQ}$ slope under $4XCO_2$, the SR_{ITCZ} decreases in all models resulting in the contraction of WA_{ITCZ}.

We speculate that the enhanced EFF_{AHT} under $4XCO_2$ (i.e., reduced slope between ITCZ location and AHT_{EQ}) is a consequence of enhanced GMS of the tropical atmosphere (Chou & Chen, 2010; Ma et al., 2012). The ensemble average stream function during the solstitial seasons (Figures 4a an 4b) achieves the slightly larger magnitude AHT_{EQ} (red arrows) energetically required in the $4XCO_2$ simulations, despite having

a weaker Ψ_{EQ}. One of many definitions of the GMS in the literature is the ratio of the moist static energy (MSE) flux by the Hadley cell divided by the mass flux (Held, 2001). This definition reduces to (C_p times) the equivalent potential temperature contrast between the upper and lower levels if the flow is concentrated in narrow layers on the upper and lower boundaries (Hill et al., 2015). We analyze this relationship by way of the seasonal regression between the tropical mass overturning stream function and atmospheric energy transport in each model (see Figure S3 in the supporting information). The inferred equivalent potential temperature contrast between the upper and lower branches (GMS) of the Hadley cell based on the seasonal slope between AHT_{EQ} and Ψ_{EQ} increases in all but one climate model under $4XCO_2$ (statistically significant at the 99.9% confidence interval). The ensemble average inferred GMS_{EQ} increases from 9.7 to 10.8 K under $4XCO_2$ (Figure S3) which amounts to a 10% change that more than accounts for the 5% ensemble average decrease in SR_{ITCZ}. This finding is consistent with the enhanced GMS of the tropical atmosphere associated with a rising tropopause (Lorenz & DeWeaver, 2007; Wu & Tan, 2013). We note that this analysis neglects the contribution of eddy MSE fluxes to GMS changes since the eddy contribution to AHT_{EQ} is included in our calculations but should be excluded from the evaluation of GMS.

As a consequence of the enhanced EFF_{AHT}, the magnitude of Ψ_{EQ} during the solstitial seasons is reduced, which manifests as an equatorward and upward shift of the Hadley cell core (cf. the solid and dashed contours in the upper panels of Figure 4). The solstitial precipitation maxima (black lines) are colocated with the maximum upward velocities and shift equatorward with the Hadley cell under global warming. The annual average of these robust seasonal results is an equatorward contraction of the region of heavy precipitation.

5. Discussion

We argue that two distinct types of tropical precipitation biases exist in models that are orthogonal in both their impact on the meridional structure of precipitation and their underlying mechanism: (1) the well-known amplitude contrast of tropical precipitation between the two hemispheres associated with the annual mean ITCZ location (Hwang & Frierson, 2013) that results from the preferential annual mean heating of the NH in the observations (Frierson et al., 2013; Marshall et al., 2013) and (2) the WA_{ITCZ} or meridional distance between the tropical precipitation peaks in the NH and SH—that is, the double ITCZ—which is intimately connected to SR_{ITCZ} and is governed by the amplitude of seasonal energy input to the atmosphere (and the efficiency of cross-equatorial heat transport). Climate models are biased toward amplified hemispheric contrast of seasonal energy input to the atmosphere resulting in overly expansive tropical wet regions. These model biases work in concert with the annual mean energetic arguments previously identified in the literature, but it is unclear which is more problematic in accurately representing the mean state of the tropics in climate models; an understanding of the root cause of biases in the seasonal cycle is paramount for future progress in reducing climate model mean state biases.

The robust meridional contraction of tropical precipitation under global warming (Lau & Kim, 2015; Su et al., 2017) results from enhanced EFF_{AHT} that is consistent with the increased GMS of the tropics—as indicated by the seasonal regression coefficient between AHT_{EQ} and Ψ_{EQ} (Figure S3). Other studies (Byrne & Schneider, 2016a, 2016b; Chou et al., 2009) have identified changes in GMS as critical to future narrowing of convective zones from annual mean energetic considerations. We offer a complementary view point that changes in the seasonal range of the ITCZ demanded by seasonal energetics and the increase in GMS_{EQ} are an essential ingredient of future tropical precipitation changes. Future changes in GMS are uncertain due to competing effects from increases in the vertical moisture gradient in the lower troposphere (Arnold et al., 2013), raising the upper branch of the circulation (with tropopause lifting) toward higher equivalent potential temperatures (Wu & Tan, 2013) and changes in the vertical structure of the meridional winds (Wei & Bordoni, 2018). Theory suggests that GMS is controlled by the SST gradient between the ITCZ and the location of interest (Hill et al., 2015) and that regions that are cooler then the SST near the ITCZ should have enhanced GMS (Merlis et al., 2013). However, this relationship is not seen in the observed spatial variability (Back & Bretherton, 2006; Inoue & Back, 2017).

Another possible explanation for the increase in EFF_{AHT} under global warming is that transient eddy moisture fluxes in the lower troposphere contribute more to AHT_{EQ} in a warmer world and, therefore, compliment the atmospheric heat transport away from the ITCZ requiring less Hadley cell shift to accomplish the same AHT_{EQ}. While eddies play a smaller role than the meridional overturning circulation (MOC) in the observed seasonal cycle of AHT_{EQ} (Figure S4), ongoing work indicates that eddies contribute more to

AHT_{EQ} in climate models and that contribution increases with global warming. The role of transient eddy moisture fluxes in ITCZ dynamics has previously been discussed by Nolan et al. (2010) and Peters et al. (2008).

The robust precipitation contraction is in stark contrast to the uncertainty in meridional shifts of the ITCZ under global warming (Donohoe & Voigt, 2015) that primarily result from the unknown structure of cloud feedbacks. Our results suggest that changes in EFF_{AHT} result from modifications of GMS linked to global mean temperature and imply that seasonal migrations of the ITCZ should increase in a cooler climate to balance the seasonal energy input to the summer hemisphere with reduced EFF_{AHT}. Thus, tropical precipitation is expected to expand meridionally during glacial periods and, as will be argued in a subsequent study, models confirm this expectation. The meridional expansion of tropical precipitation may provide an alternative interpretation of glacial hydroclimate changes deduced from the paleoclimate record which have most commonly been interpreted in terms of meridional shifts in the ITCZ (Arbuszewski et al., 2013; McGee et al., 2014; Pahnke et al., 2007; Schneider et al., 2014).

Acknowledgments
All climate model data were downloaded from the Earth System Grid Federation (ESGF) node hosted by Lawrence Livermore National Laboratory. The authors are grateful to all those who made the RCP8.5 modeling data open for public access and to all the modeling groups who participated in the CMIP5 project. Please see the supporting information for sources of observational based data. A. D. and A. R. A. were funded by the National Science Foundation Paleo Perspective on Climate Change (P2C2) Grant AGS-1702827.

References

Adam, O., Bischoff, T., & Schneider, T. (2016). Seasonal and interannual variations of the energy flux equator and ITCZ. Part I: Zonally averaged ITCZ position. *Journal of Climate*, *29*(9), 3219–3230.

Arbuszewski, J. A., deMenocal, P. B., Cleroux, C., Bradtmiller, L., & Mix, A. (2013). Meridional shifts of the Atlantic Intertropical Convergence Zone since the Last Glacial Maximum. *Journal of the Atmospheric Sciences*, *6*, 959–962.

Arnold, N., Kuang, Z., & Tziperman, E. (2013). Enhanced MJO-like variability at high SST. *Journal of Climate*, *26*, 988–1001.

Back, L. E, & Bretherton, C. S. (2006). Geographic variability in the export of moist static energy and vertical motion profiles in the tropical Pacific. *Geophysical Research Letters*, *33*, L17810. https//doi.org/10.1029/2006GL026672

Bordoni, S., & Schneider, T. (2008). Monsoons as eddy-mediated regime transitions of the tropical overturning circulation. *Nature Geoscience*, *1*, 515–519.

Byrne, M., & Schneider, T. (2016a). Narrowing of the ITCZ in a warming climate: Physical mechanisms. *Geophysical Research Letters*, *43*, 11,350–11,357. https//doi.org/10.1002/2016GL070396

Byrne, M., & Schneider, T. (2016b). Energetic constraints on the width of the Intertropical Convergence Zone. *Journal of Climate*, *29*, 4709–4721.

Chiang, J. C. H., & Friedman, A. R. (2012). Extratropical cooling, interhemispheric thermal gradients, and tropical climate change. *Annual Review of Earth and Planetary Sciences*, *40*, 383–412.

Chou, C., & Chen, C. (2010). Depth of convection and the weakening of tropical circulation in global warming. *Journal of Climate*, *23*, 3019–3030.

Chou, M. D., Neelin, J., Chen, C., & Tu, J. (2009). Evaluating the "rich-get-richer" mechanism in tropical precipitation change under global warming. *Journal of Climate*, *22*, 1982–2005.

Czaja, A., & Marshall, J. (2006). The partitioning of poleward heat transport between the atmosphere and the ocean. *Journal of the Atmospheric Sciences*, *63*, 1498–1511.

Donohoe, A., Armour, K., Pendergrass, A. G., & Battisti, D. S. (2014). Shortwave and longwave contributions to global warming under increasing CO_2. *Proceedings of the National Academy of Sciences of the United States of America*, *111*(47), 16,700–16,705.

Donohoe, A., & Battisti, D. S. (2013). The seasonal cycle of atmospheric heating and temperature. *Journal of Climate*, *26*(14), 4962–4980.

Donohoe, A., Frierson, D. M. W., & Battisti, D. S. (2013). The effect of ocean mixed layer depth on climate in slab ocean aquaplanet experiments. *Climate Dynamics*, *26*, 1041–1055. https//doi.org/10.1007/s00382-013-1843-4

Donohoe, A., Marshall, J., Ferreira, D., Armour, K., & McGee, D. (2013). The inter-annual variability of tropical precipitation and inter-hemispheric energy transport. *Journal of Climate*, *27*(9), 3377–3392.

Donohoe, A., Marshall, J., Ferreira, D., & McGee, D. (2013). The relationship between ITCZ location and atmospheric heat transport across the equator: From the seasonal cycle to the Last Glacial Maximum. *Journal of Climate*, *26*(11), 3597–3618.

Donohoe, A., & Voigt, A. (2015). Shifts in the region of tropical precipitation under global warming. In S. Wang, J. H. Yoon, R. Gillies, & C. Funk (Eds.), *Patterns of climate extremes;trends and mechanisms*. Hoboken, NJ: John Wiley and Sons.

Dwyer, J., Biasutti, M., & Sobel, A. (2012). Projected changes in the seasonal cycle of surface temperature. *Journal of Climate*, *25*, 6359–6374.

Frierson, D. M. W., & Hwang, Y.-T. (2012). Extratropical influence on ITCZ shifts in slab ocean simulations of global warming. *Journal of Climate*, *25*, 720–733.

Frierson, D. M. W, Hwang, Y. T., Fuckar, N. S., Seager, R., Kang, S. M., Donohoe, A., et al. (2013). Why does tropical rainfall peak in the Northern Hemisphere? The role of the oceans meridional overturning circulation. *Nature Geoscience*, *6*, 940–944.

Hadley, G. (1735). Concerning the cause of the general tradewinds. *Philosophical Transactions of the Royal Society A*, *29*, 58–62.

Held, I. M. (2001). The partitioning of the poleward energy transport between the tropical ocean and atmosphere. *Journal of the Atmospheric Sciences*, *58*, 943–948.

Hill, S., Ming, Y., & Held, I. (2015). Mechanisms of forced tropical meridional energy flux change. *Journal of Climate*, *28*, 1725–1742.

Hu, Y., Li, D., & Liu, J. (2007). Abrupt seasonal variation of the ITCZ and Hadley circulation. *Geophysical Research Letters*, *34*, L18814. https//doi.org/10.1029/2007GL030950

Huang, P., Xie, S. P., Hu, K., Huang, G., & Huang, R. (2013). Patterns of the seasonal response of tropical rainfall to global warming. *Nature Geoscience*, *6*(5), 357–361. https//doi.org/10.1038/ngeo1792

Hwang, Y. T., & Frierson, D. M. W. (2013). Link between the double-Intertropical Convergence Zone problem and cloud bias over Southern Ocean. *Proceedings of the National Academy of Sciences of the United States of America*, *110*, 4935–4940.

Inoue, K., & Back, L. E. (2017). Gross moist stability analysis: Assessment of satellite-based products in the GMS plane. *Journal of the Atmospheric Sciences*, *74*, 1819–1837.

Johanson, C. M., & Fu, Q. (2009). Hadley cell widening: Model simulations versus observations. *Journal of Climate*, *22*, 2713–2725.

Kang, S. M., Held, I. M., Frierson, D. M. W., & Zhao, M. (2008). The response of the ITCZ to extratropical thermal forcing: idealized slab-ocean experiments with a GCM. *Journal of Climate*, *21*, 3521–3532.

Lau, W., & Kim, K. (2015). Robust Hadley circulation changes and increasing global dryness due to CO_2 warming from CMIP5 model projections. *Proceedings of the National Academy of Sciences of the United States of America*, *122*, 3630–3635.

Lindzen, R. S., & Hou, A. Y. (1988). Hadley circulations of zonally averaged heating centered off the equator. *Journal of the Atmospheric Sciences*, *45*(17), 2416–2427.

Lorenz, D., & DeWeaver, E. (2007). Tropopause height and zonal wind response to global warming in the IPCC scenario integrations. *Climate Dynamics*, *112*, D10119.

Ma, J., Xie, S., & Kosaka, Y. (2012). Mechanisms for tropical tropospheric circulation change in response to global warming. *Journal of Climate*, *25*, 2979–2994.

Marshall, J., Donohoe, A., Ferreira, D., & McGee, D. (2013). The oceans role in setting the mean position of the Intertropical Convergence Zone. *Climate Dynamics*, *14*, 1967–1979. https//doi.org/10.1007/s00382-013-1767-z

McGee, D., Donohoe, A., Marshall, J., & Ferreira, D. (2014). Changes in tropical precipitation, ITCZ location and hemispheric energy budgets at the Last Glacial Maximum, Heinrich Stadial 1, and the mid-Holocene. *Earth and Planetary Science Letters*, *390*, 69–79.

Merlis, T. M., Schneider, T., Bordoni, S., & Eisenman, I. (2013). Hadley circulation response to orbital precession. Part I: Aquaplanets. *Journal of Climate*, *26*(3), 740–753.

Nolan, D. S., Powell, S. W., Zhang, C., & Mapes, B. E. (2010). Idealized simulations of the Intertropical Convergence Zone and its multilevel flows. *Journal of the Atmospheric Sciences*, *67*, 4028–4053.

Pahnke, K., Sachs, J. P., Keigwin, L., Timmerman, A., & Xie, S. P. (2007). Eastern tropical Pacific hydrologic changes during the past 27,000 years from D/H ratios in alkenones. *Paleoceanography*, *22*, PA4214. https://doi.org/10.1029/2007PA001468

Peters, M. E., Kuang, Z., & Walker, C. C. (2008). Analysis of atmospheric energy transport in ERA-40 and implications for simple models of the mean tropical circulation. *Journal of Climate*, *21*, 5229–5241.

Popp, M., & Lutsko, N. J. (2017). Quantifying the zonal-mean structure of tropical precipitation. *Geophysical Research Letters*, *44*, 9470–9478. https//doi.org/10.1002/2017GL075235

Quan, X.-W., Hoerling, M. P., Perlwitz, J., Diaz, H. F., & Xu, T. (2014). How fast are the Tropics expanding? *Journal of Climate*, *27*, 1999–2013.

Roberts, W. H. G., Valdes, P. J., & Singarayer, J. S. (2017). Can energy fluxes be used to interpret glacial/interglacial precipitation changes in the tropics? *Geophysical Research Letters*, *44*, 6373–6382. https//doi.org/10.1002/2017GL073103

Sachs, J. P., Sachse, D., Smittenberg, R. H., Zhang, Z., Battisti, D. S., & Golubic, S. (2009). Southward movement of the Pacific intertropical convergence zone AD 1400–1850. *Nature Geoscience*, *2*, 519–525.

Schneider, T, Bischoff, T., & Haug, G. H. (2014). Migrations and dynamics of the Intertropical Convergence Zone. *Nature*, *513*, 45–53.

Su, H., Jiang, J. H., Neelin, D., Shen, J., Zhai, C., Yue, Q., et al. (2017). Tightening of tropical ascent and high clouds key to precipitation change in a warmer climate. *Nature Communications*, *8*, 15771.

Taylor, K. E., Stouffer, R. J., & Meehl, G. A. (2012). An overview of CMIP5 and the experiment design. *Bulletin of the American Meteorological Society*, *93*, 485–498.

Waugh, D., Garfinkel, C., & Polvani, L. (2015). Drivers of the recent tropical expansion in the Southern Hemisphere. *Journal of Climate*, *28*, 6581–6586.

Wei, H.-H., & Bordoni, S. (2018). Energetic constraints on the ITCZ position in idealized simulations with a seasonal cycle. *Journal of Advances in Modeling Earth Systems*, *10*, 1708–1725. https//doi.org/10.1029/2018MS001313

Wodzicki, K., & Rapp, A. (2016). Long term characterization of the Pacific ITCZ using TRMM, GPCP, and ERA-Interim. *Journal of Geophysical Research: Atmospheres*, *121*, 3153–3170. https//doi.org/10.1002/2015JD024458

Wu, T., & Tan, P. (2013). Changes in gross moist stability in the tropics under global warming. *Climate Dynamics*, *41*, 2481–2496.

Xian, P., & Miller, R. L. (2008). Abrupt seasonal migration of the ITCZ into the summer hemisphere. *Journal of the Atmospheric Sciences*, *65*, 1678–1695.